

Electrode shape modification for efficient dye removal using electrocoagulation

S. M. Al-Mahmoud

Department of Chemistry, College of Education for Women, Tikrit University, Tikrit, 34001, Iraq

Received: October 07, 2025; Revised: December 05, 2025

The electrode configuration can strongly influence the electrocoagulation removal performance. This study aimed to introduce a new aluminum-based curved plate (AICP) electrode to improve the electrocoagulation process as a treatment method for Eriochrome black T-contaminated water. Different factors influencing the electrocoagulation process, such as coagulation time, applied voltage, initial dye concentration, electrode distance, and operating temperature, were investigated. The superior removal efficiency of 97% was acquired at 105 min removal time, 30 V applied voltage, 1 cm electrode distance, 80 mg/L initial EBT concentration, and 318 K operating temperature. The findings emphasize that the removal efficiency of EBT dye increased with increasing coagulation time, applied voltage, initial dye concentration, and operating temperature, and it decreased with increasing the distance between electrodes. The kinetic investigation revealed that the pseudo-second order adsorption model properly described the removal process. In addition, the comparison between the new curved plate electrodes and the conventional flat plate electrodes under the same operating conditions revealed that the maximum removal efficiency of 97% was obtained for the new aluminum-based curved plate (AICP) electrodes compared to 90% for the conventional flat plate electrodes. This higher removal efficiency is due to the curved structure of the electrodes, which helps to improve flow hydrodynamics and mass transfer, thus reducing the removal time.

Keywords: Electrocoagulation, Curved electrode, Electrode modification, Eriochrome black T.

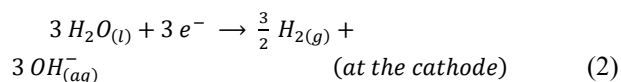
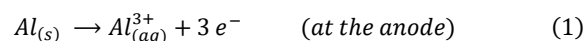
INTRODUCTION

Aquatic systems are exposed to numerous activities, caused by human beings, that alter their intrinsic nature. One of these primary activities is the disposal of colored materials, resulting from industrial processes, into water bodies [1]. Dyes are organic compounds that have a negative influence on aquatic organisms due to their durability, toxicity, and low biodegradability [2, 3]. Eriochrome black T (EBT) is an anionic azo dye that is exceedingly utilized in the textile industry [4]. It was recently reported that prolonged exposure to EBT can cause carcinogenic and toxic effects to the aquatic environment [5]. Therefore, eliminating EBT from contaminated water before discharging to water bodies is substantial.

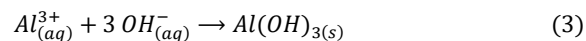
Among the major methods used for dye treatment in wastewater, electrocoagulation (EC) can be considered a promising technique for water treatment due to its unique properties, such as operation simplicity, process efficiency, and various contaminants removal ability [6, 7]. However, some limitations hinder its wide spread, such as sludge production, energy consumption, and electrode corrosion [8, 9].

Electrocoagulation merges the advantages of coagulation, flotation, sedimentation, and electrochemical oxidation processes [10]. Its

working principle is based on the formation of a coagulant as a result of the current flows through the metal electrodes flooded in the sample solution [11]. The metal cations produced from the surface of the anode electrode (Eq. 1) associate with the hydroxyl ions released from the water reduction at the cathode electrode (Eq. 2), to form metal hydroxides (Eq. 3) [12]. The reactions occurring on the aluminum electrodes are as follows [10–12]:



The hydroxyl formation through the EC process is:



$Al(OH)_3$ has a large surface area, which is of great benefit in the rapid adsorption of dissolved compounds and trapping of colloidal particles [16]. It works as a coagulant to destabilize the polluting particles and leads to the formation of larger particles that are easier to separate and remove from the water through sedimentation or by flotation to the surface with hydrogen gas bubbles liberated at the cathode [17].

Recent studies by Mohan *et al.* concluded that the maximum removal efficiency about 98% of Congo

* To whom all correspondence should be sent:
Email: s_almahmoud@tu.edu.iq

red [18], and 99% of EBT [19] was achieved using copper electrodes in an electrocoagulation process. The investigation of Kalivel *et al.* [20] disclosed that aluminum electrodes are preferable to copper electrodes in removing Red BFL dye. Bendaia *et al.* [21] showed 95% removal efficiency of Acid red 14 using planar aluminum electrodes. Yazdandoust *et al.* [22] applied planar aluminum electrodes for the elimination of Direct red 80 from polluted water, and only 89.3% of the dye removal was achieved with the assistance of *Moringa oleifera* seed extract.

The hydrodynamics and the mass transport in major electrocoagulation cells that use normal planar plate electrodes are not very efficient [23]. The planar plate electrodes can act as a barrier disturbing the flow dynamics that can reduce the degree of homogenization in the solution [24]. Also, the generated gas bubbles can act as an electrical shield of the electrode nucleation sites that significantly affect the current distribution and the electrolyte conductivity [25]. Therefore, to overcome these obstacles, some literature reported the use of an alternative strategy based on improving the electrode design, such as a perforated plate electrode [26], rotating electrode [27], rotating cylindrical electrode [28], folded plate electrode [29], cubic electrodes [30], spiral electrode [31], which can enhance mixing efficiency and mass transport rates and thus promote uniform current distribution [32, 33].

The novelty of this paper consists of using two Al-based parallel curved plate (AICP) electrodes in the electrocoagulation technique to remove EBT from a synthetic aqueous solution. The influence of electrode shape, treatment time, electrode distance, applied voltage, process temperature, and initial dye concentration was examined in terms of EBT removal from aqueous media.

EXPERIMENTAL

Eriochrome black T (EBT) of analytical grade was obtained from Fluka and used as received without any treatment. Its chemical formula is $C_{20}H_{12}N_3NaO_7S$, m. wt. 463.381 g/mol, and its λ_{max} is about 530 nm [34].

The electrocoagulation experiments were performed in a 250-mL cylindrical cell. The experimental setup of the electrocoagulation process is illustrated in Fig. 1. The experiments were carried out using a DC power supply (Dazheng, 0-30 V, China), 8-tube centrifuge (Gallenkamp, England), and ultraviolet-visible spectroscopy (UV-1800, Shimadzu, Japan). The experiments were conducted using 200 mL of a dye solution prepared by dissolving EBT in distilled water to obtain the desired EBT concentration.

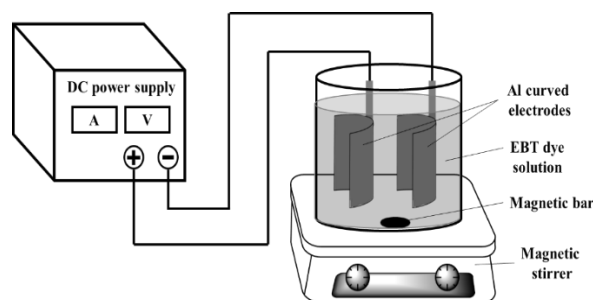


Fig. 1. Schematic experimental setup of the electrocoagulation system.

A pair of aluminum-based parallel curved plate (AICP) electrodes (Fig. 2a) with dimensions of 4 cm length, 5 cm width, and 0.6 cm thickness, with an effective surface area of 20 cm², was immersed in the dye solution in the cylindrical cell. The electrodes were connected through a copper wire to a DC power supply. For comparison, a pair of aluminum-based flat plate (AIFP) electrodes (Fig. 2b) with the same dimensions was also utilized. The electrocoagulation cell before and after the removal process is presented in Figs. 2c and 2d, respectively.

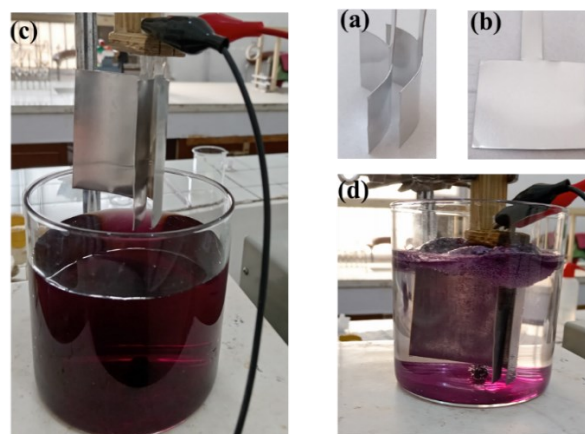


Fig. 2. AICP electrode (a), AIFP electrode (b), the cylindrical cell before (c) and after (d) electrocoagulation.

The effect of different factors on the EBT removal efficiency by the electrocoagulation process was tested. Each experiment was performed by varying one factor and keeping the others constant to obtain the optimal removal circumstances. These factors are removal time (15, 30, 45, 60, 75, 90, 105, and 120 min), applied voltage (10, 20, 30 V), electrode distance (1, 2, 3 cm), temperature (298, 308, 318 K), and initial EBT concentration (20, 40, 60, 60, and 80 mg/L). The solutions were separated at 3000 rpm in an 8-tube centrifuge to obtain a clear residual EBT dye supernatant whose absorbance was measured by ultraviolet-visible spectroscopy at 530 nm.

The values of the removal efficiency (% Removal) and adsorption capacity (q_e) were estimated using Eqs. 4 and 5, respectively [18].

$$\% \text{ Removal} = \frac{A_0 - A_t}{A_0} \times 100 \quad (4)$$

$$q_e = \frac{(C_0 - C_e)V}{m} \quad (5)$$

where A_0 is the solution absorbance before electrocoagulation and A_t is the solution absorbance after electrocoagulation, C_0 and C_e represent the initial concentration and the equilibrium concentration (mg/L), respectively, V is the volume of the dye solution (L), and m is the amount of electrode consumption (g).

The energy consumption (C_{energy}) and electrode consumption ($C_{\text{electrode}}$) depending on Faraday's law, were calculated using Eqs. 6 and 7, respectively [17, 19].

$$C_{\text{energy}} = U I t \quad (6)$$

$$C_{\text{electrode}} = \frac{M I t}{n F} \quad (7)$$

where U is the applied voltage (V), I is the electric current (A), t is the electrolysis time (s), M is the aluminum molar mass (26.98 g/mol), n is the number of transferred electrons, and F is Faraday constant (96487 C/mol).

The kinetic study of the AICP electrodes was performed by applying two kinetic models, the pseudo-first order (Eq. 8) and the pseudo-second order (Eq. 9) [18],

$$\ln(q_e - q_t) = \ln q_e - k_1 t \quad (8)$$

$$\frac{t}{q_t} = \frac{1}{k_2 q_e^2} + \frac{t}{q_e} \quad (9)$$

where q_e and q_t represent the adsorption capacity at equilibrium and at time (t), respectively, k_1 and k_2 are the pseudo-first and the pseudo-second order rate constants.

RESULTS AND DISCUSSION

The influence of electrocoagulation time on the removal of EBT dye from aqueous media using AICP electrodes was investigated using removal time intervals (15, 30, 45, 60, 75, 90, 105, and 120 min), applied voltage 30 V, electrode distance 1 cm, temperature 298 K, and initial EBT concentration 20 mg/L. Fig. 3 shows that a lower removal efficiency of about 68% occurs at the beginning of the electrocoagulation process. Increasing the process time increases the removal efficiency to achieve its maximum value of about 97% in about 105 min. In addition, as the electrolysis time increases from 15 to 105 min, the energy consumption rises from 0.225 kWh to 1.575 kWh, along with electrode consumption from 0.0025 g to 0.0176 g. This can be

explained by considering that increasing the removal time will increase the release of Al^{3+} ions at the anode (Eq. 1) and of hydroxyl ions at the cathode (Eq. 2), which can lead to the production of an additional amount of aluminum hydroxide that promotes the adsorption of more dye molecules. Moreover, the improved mixing and hydrodynamic flow provided by the AICP electrodes can create more opportunities for interaction to occur between the produced coagulant and the dye particles, thereby improving the contaminant removal efficiency during the electrocoagulation process. Hashim *et al.* [26] explained that the treatment time exerts an important effect on the removal efficiency and reported that increasing the electrolysis time from 5 to 30 min using aluminum baffle-plate electrodes can enhance the removal efficiency of *Escherichia coli* by 60%. Hawari *et al.* [35] reported that about 19.6% of the total organic carbon removal was achieved in 5 min using symmetrical aluminum electrodes compared to 67.7% in 60 min, and they claimed that changing the electrode configuration by introducing asymmetrical aluminum electrodes can enhance the removal efficiency to 87.7%.

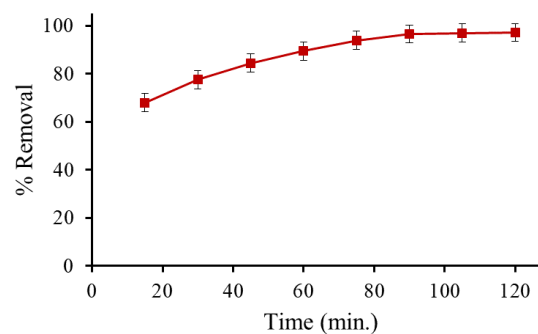


Fig. 3. EBT removal with time using AICP electrodes

The operation potential is a crucial factor that has an essential impact on the electrocoagulation process. Fig. 4 displays the EBT dye removal using AICP electrodes at various applied voltages (10, 20, and 30 V), electrode distance 1 cm, temperature 298 K, and initial EBT concentration of 20 mg/L. It shows that increasing the applied voltages from 10 V to 30 V increases the removal efficiency from 72% to 97%. This proves that the higher the potential, the greater is the electrocoagulation efficiency. Gasmi *et al.* [17] reported that better removal efficiency can be achieved at a higher voltage. Increasing the potential leads to an increase in the electric current flowing through the cell. According to Faraday's law (Eq. 7), the amount of dissolved material from the electrodes is proportional to the amount of current flowing through them. Therefore, increasing the electric voltage contributes to the dissolution of the

aluminum electrodes, which leads to the release of larger quantities of Al^{3+} ions that react with water to form aluminum hydroxide flocs which have a high capacity to absorb and clump dye molecules [14]. In addition, increasing the electrical voltage also contributes to the generation of larger quantities of hydrogen gas bubbles at the cathode, resulting from the decomposition of water, which in turn contributes to raising pollutant particles to the surface *via* electroflotation [36].

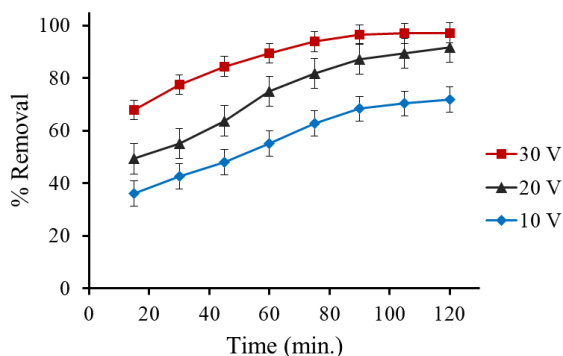


Fig. 4. EBT removal with time at different voltages using AICP electrodes.

The effect of the distance between the electrodes was also studied using three electrode distances (1, 2, and 3 cm), applied voltage 30 V, temperature 298 K, and initial EBT concentration of 20 mg/L. It can be seen from Fig. 5 that the highest removal efficiency of 97% is achieved using 1 cm distance. Increasing the distance between the electrodes to 3 cm lowers the removal efficiency to about 84%. Also, a decrease in the electrode consumption from 0.0176 g to 0.0058 g occurs as the electrode distance increases from 1 cm to 3 cm. This is due to the increase in the solution resistance and thus decrease of electrical conductivity that reduces the generation of coagulant particles and hydrogen bubbles necessary for dye removal. Mohan *et al.* [18] reported that inter-electrode distance plays a critical role in the removal process, and the removal efficiency was enhanced by about 9% on decreasing the electrode distance from 3 cm to 0.5 cm.

The operating temperature has a key role in the electrocoagulation performance. This study examined different temperatures (298, 308, 318 K), using 30 V applied voltage, electrode distance 1 cm, and initial EBT concentration of 20 mg/L.

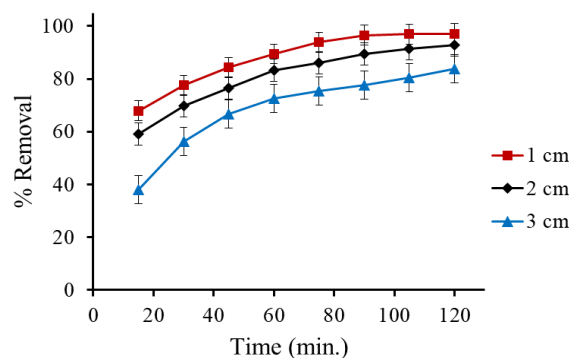


Fig. 5. EBT removal with time at different electrode distances using AICP electrodes.

At the early stages of the electrocoagulation process, the removal efficiency is affected by the changes in the temperature, significantly increasing with increasing temperature, as shown in Figure 6. However, there is no considerable effect after 100 min since the electrocoagulation process has reached the final stage. It is well-known that raising the operating temperature usually increases the electrocoagulation efficiency [37]. Increasing the temperature would enhance the solution conductivity and ionic mobility as a result of the reduction in the solution resistance and viscosity [24], allowing a higher current flow that would accelerate the electrochemical reactions at the electrodes and thus facilitate coagulant generation. Mohan *et al.* [19] explained that raising the temperature can enhance the ionic mobility as a result of the increase in the kinetic energy of each molecule, and removal efficiency can be enhanced by 29% through raising the temperature from 313 K to 348 K. Al-Raad *et al.* [27] reported that about 4% of the removal efficiency was obtained by increasing the temperature from 298 K to 318 K.

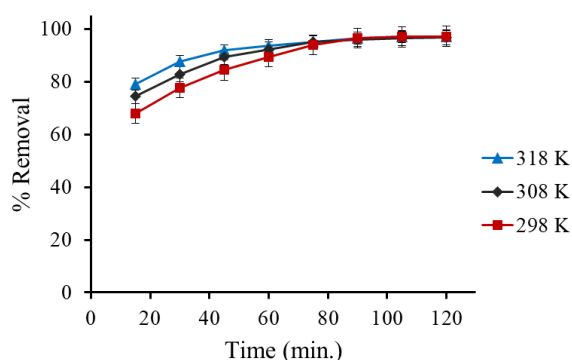


Fig. 6. EBT removal with time at different temperatures using AICP electrodes.

The influence of initial EBT concentration on the removal efficiency of the electrocoagulation process utilizing AICP electrodes was also investigated using initial EBT concentrations of 20, 40, 60, 60, and 80 mg/L, applied voltage 30 V, electrode distance 1 cm, and temperature of 298 K. A clear difference in the removal efficiency can be noticed at the beginning of the removal process, as illustrated in Fig. 7. As the initial EBT concentration rises from 20 mg/L to 80 mg/L, the removal efficiency increases from 68% to 96%. At higher dye concentration, there will be more dye molecules in the solution. This increases the probability of collision and interaction with the generated aluminum hydroxide coagulants. As a result, it enhances the aggregation and floc formation. Moreover, many dyes are charged, and a higher concentration increases the ionic strength of the solution, which helps neutralize charges more effectively and promotes coagulation/flocculation, thereby enhancing the efficient removal of the dye. On the other hand, the removal efficiencies are almost identical after 100 min at all concentrations used, which can be attributed to the electrocoagulation process being close to reaching the final stage. Bazrafshan *et al.* [38] attributed the significant reduction in removal efficiency at lower initial concentration to the dilute solution theory. The diffusion layer formed around the electrode in a dilute solution causes a slower reaction rate, while the diffusion layer in the concentrated solution has no impact on the rate of migration of metal ions to the surface of the electrode. Kausleya *et al.* [39] reported that only 70% reduction was achieved at a lower initial TOC concentration, while 91% drop was obtained for a higher initial TOC concentration. They explained that a higher initial concentration can increase the collision rate between the pollutant molecules and with the produced coagulants that reduces the pollutant content in the solution.

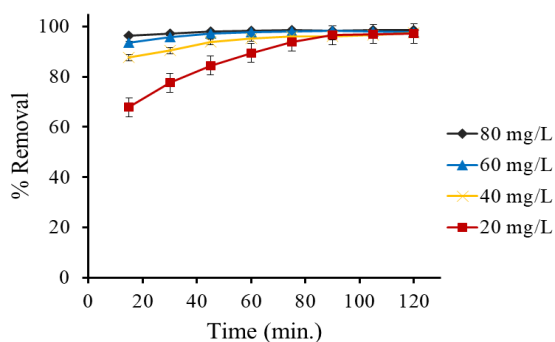


Fig. 7. EBT removal with time at different initial EBT concentrations using AICP electrodes.

The kinetic study of the AICP electrodes was carried out by applying the pseudo-first order (Eq. 8) and the pseudo-second order (Eq. 9) adsorption models to the data obtained from the removal time experiment under the optimized conditions. Fig. 8 shows the plots of these two models, and their calculated parameters are presented in Table 1. It can be clearly seen that the highest correlation coefficient of 0.99 was achieved by the pseudo-second order adsorption model compared to 0.88 for the pseudo-first order adsorption model. Also, the theoretical adsorption capacity of the pseudo-second order adsorption model is the closest value to the experimental adsorption capacity. These findings prove that the kinetic study results are more consistent with the pseudo-second order adsorption model, which confirms a chemical adsorption of EBT dye molecules on the aluminum surface.

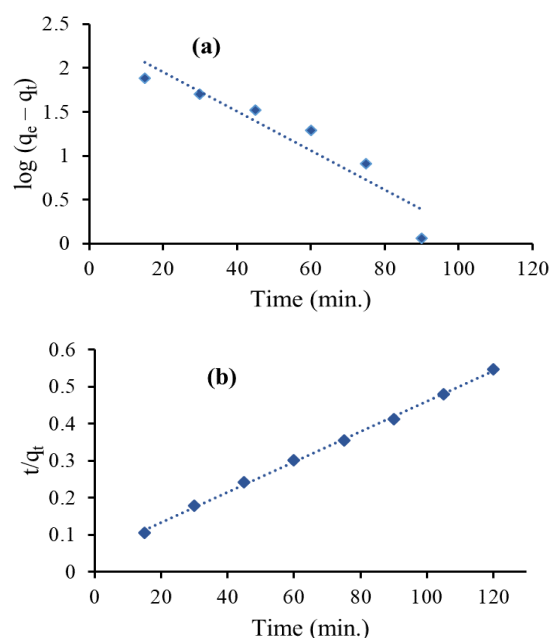


Fig. 8. Kinetic plots of (a) pseudo-first order, (b) pseudo-second order adsorption models.

Table 1. Kinetic parameters calculated for the removal process.

Kinetic model	Kinetic parameter	Value
	q_e exp. (mg. g ⁻¹)	219.1
Pseudo-first order	q_e calc. (mg. g ⁻¹)	250.8
	k_1 (min ⁻¹)	0.051
	R^2	0.88
Pseudo-second order	q_e calc. (mg. g ⁻¹)	243.9
	k_2 (g. mg ⁻¹ min ⁻¹)	0.0003
	R^2	0.99

A comparison between the traditional aluminum-based flat plate (AIFP) electrodes and the new shaped aluminum-based curved plate (AICP)

electrodes was made using removal time intervals of 15, 30, 45, 60, 75, 90, 105, and 120 min, under optimal conditions of applied voltage 30 V, electrode distance 1 cm, temperature 298 K, and initial EBT concentration of 20 mg/L. Figure 9 shows that both AIFP and AICP electrodes attained a reasonable removal efficiency of approximately 68% at the start of the elimination process. As the treatment time increases, the removal efficiency gradually increases for both electrodes. However, the AICP electrodes perform better and provide more effective removal, attaining 97% at 105 min compared to 86% of conventional AIFP electrodes. This finding can be explained by the fact that conventional AIFP electrodes can act as a barrier, disturbing the flow circulation and hindering the hydrodynamics of the flow, which reduces their performance [24, 40]. Zafar *et al.* [41] reported that using planar aluminum electrodes can eliminate about 81% and 82% of methylene blue and methyl orange, respectively. Soliman *et al.* [42] made a modification to the electrocoagulation reactor to treat ammonia-contaminated wastewater, and only 76.3% of the removal efficiency was due to the stacked aluminum disc electrode. Jafari *et al.* [31] stated that mixing is the major drawback that affects the removal efficiency in a conventional electrocoagulation reactor and the electrode configuration can play a substantial role in the electrocoagulation process. They reported that the mass transfer between the electrodes using spiral electrode configuration is anticipated to increase the removal efficiency.

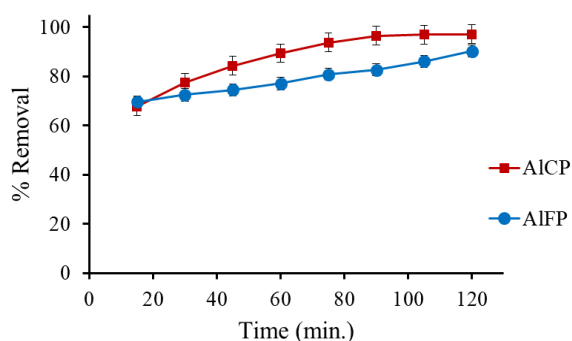


Fig. 9. EBT removal with time using AIFP and AICP electrodes.

The new AICP electrode can better promote the hydrodynamic flow. Its curved configuration, expected to enhance mixing and mass transfer, allows for rapid homogeneity of the solution and provides more opportunities for interaction to occur between coagulant flocs and EBT particles, thereby decreasing treatment time. This leads to improved contaminant removal efficiency of the

electrocoagulation process compared to conventional aluminum-based flat plate electrodes (AIFP).

CONCLUSIONS

This research aims to introduce aluminum-based curved plate electrodes in the electrocoagulation technique for enhancing the removal of EBT from aqueous media. The main factors influencing the electrocoagulation process were examined, including treatment time, applied voltage, initial EBT concentration, electrode distance, and operating temperature. The optimal removal efficiency of 97% was obtained at optimized parameters: 105 min removal time, 30 V applied voltage, 1 cm electrode distance, 80 mg/L initial EBT concentration, and 318 K operating temperature. The results confirm that the EBT dye removal efficiency increases with increasing coagulation time, applied voltage, initial dye concentration, and operating temperature, and it decreases with increasing the inter-electrode distance. The pseudo-second order adsorption model provides a better fit to the experimental data of the removal process. A comparison was made between the new curved plate electrodes and the traditional flat plate electrodes under the optimized operating conditions. Efficient removal of EBT from aqueous solution was accomplished by the new aluminum-based curved plate (AICP) electrodes, which can be attributed to their curved shape that promotes mixing and mass transfer, allowing for rapid homogeneity of the solution to take place, which increases the removal efficiency of the electrocoagulation process. These findings emphasize that the new aluminum-based curved plate (AICP) electrodes can be adopted in the electrocoagulation technology.

Acknowledgement: The author thanks the Department of Chemistry, College of Education for Women, Tikrit University, for supporting this research.

REFERENCES

1. H. B. Rahmoun, M. Boumediene, A. N. Ghenim, E. F. da Silva, J. Labrincha, *Environments*, **12**, 1 (2025).
2. I. A. W. Khalaf, S. M. Al-Mahmoud, *Macromol. Symp.*, **414**, 2400223 (2025).
3. S. M. Al-Mahmoud, *Eurasian Chem. J.*, **27**, 219 (2025).
4. W. Boumya, M. Khnifira, A. Machrouhi, M. Abdennouri, M. Sadiq, M. Achak, G. Serdaroğlu, S. Kaya, S. Şimşek, N. Barka, *J. Mol. Liq.*, **331**, 115706 (2021).
5. S. Karishma, V. C. Deivayanai, P. Thamarai, A. Saravanan, P. R. Yaashikaa, *Sustain. Chem. Environ.*, **7**, 100143 (2024).

6. M. Kobya, P. I. Omwene, S. M. Sarabi, S. Yildirim, Z. Ukundimana, *Process Saf. Environ. Prot.*, **152**, 188 (2021).
7. P. V. Nidheesh, Ö. Gökkuş, *Chemosphere*, **310**, 2021 (2023).
8. A. A. Moneer, N. M. El-Mallah, M. M. El-Sadaawy, M. Khedawy, M. S. H. Ramadan, *Desalin. Water Treat.*, **256**, 300 (2022).
9. J. T. Jose, K. L. Priya, S. Chellappan, S. Sreelekshmi, A. Remesh, V. Venkidesh, A. J. Krishna, A. Pugazhendhi, S. Selvam, V. Baiju, M. S. Indu, *Environ. Res.*, **252**, 118759 (2024).
10. M. Mousazadeh, E. K. Niaragh, M. Usman, S. U. Khan, M. A. Sandoval, Z. Al-Qodah, Z. Bin Khalid, V. Gilhotra, M. M. Emamjomeh, *Environ. Sci. Pollut. Res.*, **28**, 43143 (2021).
11. B. Biswas, S. Goel, *Chemosphere*, **302**, 134709 (2022).
12. A. Gasmi, N. Elboughdiri, D. Ghernaout, A. Hannachi, *Desalin. Water Treat.*, **271**, 74 (2022).
13. M. M. Emamjomeh, S. Kakavand, H. A. Jamali, S. M. Alizadeh, M. Safdari, S. E. S. Mousavi, K. S. Hashim, M. Mousazadeh, *Desalin. Water Treat.*, **205**, 161 (2020).
14. B. K. Zaied, M. Rashid, M. Nasrullah, A. W. Zularisam, D. Pant, L. Singh, *Sci. Total Environ.*, **726**, 138095 (2020).
15. H. Liu, Y. Wu, M. Li, H. Ma, M. Li, K. Zhu, Jian zhang, G. Chen, Z. Wang, S. Wang, *Chemosphere*, **268**, 128851 (2021).
16. N. Ungureanu, V. Vlăduț, G. Paraschiv, *Water (Switzerland)*, **3**, 206 (2019).
17. A. Gasmi, S. Ibrahim, N. Elboughdiri, M. A. Tekaya, D. Ghernaout, A. Hannachi, A. Mesloub, B. Ayadi, L. Kolsi, *ACS Omega*, **7**, 22456 (2022).
18. S. Mohan, P. Sharath, B. M. Nagabhushana, Chikkahanumantharayappa, C. Shivakumara, *Indian J. Chem.*, **61**, 1054 (2022).
19. S. Mohan, B. M. Nagabhushana, Chikkahanumantharayappa, C. Shivakumara, *Asian J. Sci. Appl. Technol.*, **10**, 5 (2021).
20. P. Kalivel, J. C. Jisson, S. Kavitha, J. Bhagavathsingh, J. Palanichamy, M. M. Stephen, J. J. David, *Int. J. Environ. Anal. Chem.*, **103**, 5619 (2021).
21. M. Bendaia, S. Hazourli, A. Aitbara, N. Merzoug, *Sep. Sci. Technol.*, **56**, 2087 (2020).
22. M. Yazdandoust, M. H. Ehrampoush, A. Dalvand, *Int. J. Environ. Anal. Chem.*, **104**, 2485 (2022).
23. A. A. Márquez, O. Coreño, J. L. Nava, *J. Electroanal. Chem.*, **911**, 116223 (2022).
24. S. Adamović, R. Milošević, M. Prica, *Desalin. Water Treat.*, **321**, 100982 (2025).
25. A. D. Villalobos-Lara, T. Pérez, A. R. Uribe, J. A. Alfaro-Ayala, J. D. J. Ramírez-Minguela, J. I. Minchaca-Mojica, *J. Electroanal. Chem.*, **858**, 113807 (2020).
26. K. S. Hashim, P. Kot, S. L. Zubaidi, R. Alwash, R. Al Khaddar, A. Shaw, D. Al-Jumeily, M. H. Aljefery, *J. Water Process Eng.*, **33**, 101079 (2020).
27. A. A. Al-Raad, M. M. Hanafiah, A. S. Naje, M. A. Ajeel, *Environ. Pollut.*, **265**, 115049 (2020).
28. A. D. Villalobos-Lara, F. Álvarez, Z. Gamiño-Arroyo, R. Navarro, J. M. Peralta-Hernández, R. Fuentes, T. Pérez, *Chemosphere*, **264**, 128491 (2021).
29. Z. Wu, J. Dong, Y. Yao, Y. Yang, F. Wei, *Environ. Technol. Innov.*, **22**, 101448 (2021).
30. F. Y. AlJaberi, Z. A. Hawaas, *MethodsX*, **10**, 101951 (2023).
31. E. Jafari, M. R. Malayeri, H. Brückner, T. Weimer, P. Krebs, *J. Environ. Manage.*, **347**, 119085 (2023).
32. P. V. Nidheesh, A. A. Oladipo, N. G. Yasri, A. R. Laiju, V. R. S. Cheela, A. Thiam, Y. G. Asfaha, S. Kanmani, E. (Ted) P. L. Roberts, *Process Saf. Environ. Prot.*, **166**, 600 (2022).
33. M. Bajpai, I. Seidu, E. Gengec, *J. Water Process Eng.*, **77**, 108637 (2025).
34. E. D. Luna, M. Daniel, G. de Flores, D. A. D. Genuino, C. M. Futralan, M. Wan, *J. Taiwan Inst. Chem. Eng.*, **44**, 646 (2013).
35. A. H. Hawari, A. M. Alkhatib, M. A. Hafiz, P. Das, *Environ. Sci. Pollut. Res.* **27**, 23888 (2020).
36. N. Muhammad Niza, N. Abdul Razak, M. S. Yusoff, M. A. A. Mohd Zainuri, M. I. Emmanuel, A. Mohamed Hussen Shadi, M. H. Mohd Hanif, M. A. Kamaruddin, *Sep. Purif. Technol.*, **258**, 118089 (2021).
37. S. Boinpally, A. Kolla, J. Kainthola, R. Kodali, J. Vemuri, *Water Cycle*, **4**, 26 (2023).
38. E. Bazrafshan, K. A. Ownagh, A. H. Mahvi, *E-Journal Chem.*, **9**, 2297 (2012).
39. S. B. Kausley, C. P. Malhotra, A. B. Pandit, *J. Water Process Eng.*, **16**, 149 (2017).
40. J. N. Hakizimana, B. Gourich, M. Chafi, Y. Stiriba, C. Vial, P. Drogui, J. Naja, *Desalination*, **404**, 1 (2017).
41. A. M. Zafar, A. Naeem, M. A. Minhas, M. J. Hasan, S. Rafique, A. Ikhlaiq, *Total Environ. Adv.*, **9**, 200087 (2024).
42. M. S. Soliman, I. M. Awaad, S. A. Nosier, M. Hussein, M. H. Abdel-Aziz, M. A. El-Naggar, *Results Eng.*, **28**, 107819 (2025).